

Swing-leg retraction: a simple control model for stable running

André Seyfarth^{1,3,*}, Hartmut Geyer^{1,3} and Hugh Herr^{1,2,4}

¹Artificial Intelligence Laboratory and ²Harvard/MIT Division of Health Sciences and Technology, Cambridge, MA 02139, USA, ³ParaCare Laboratory, Balgrist Hospital, University Zurich, CH-8008 Zurich, Switzerland and ⁴Department of Physical Medicine and Rehabilitation, Harvard Medical School, Spaulding Rehabilitation Hospital, Boston, MA 02114, USA

*Author for correspondence (e-mail: a_seyfarth@yahoo.com)

Accepted 22 February 2003

Summary

In running, the spring-like axial behavior of stance limbs is a well-known and remarkably general feature. Here we consider how the rotational behavior of limbs affects running stability. It is commonly observed that running animals retract their limbs just prior to ground contact, moving each foot rearward towards the ground. In this study, we employ a conservative spring-mass model to test the effects of swing-leg retraction on running stability. A feed-forward control scheme is applied where the swing-leg is retracted at constant angular velocity throughout the second half of the swing phase. The control scheme allows the spring-mass system to automatically

adapt the angle of attack in response to disturbances in forward speed and stance-limb stiffness. Using a return map to investigate system stability, we propose an optimal swing-leg retraction model for the stabilization of flight phase apex height. The results of this study indicate that swing-leg retraction significantly improves the stability of spring-mass running, suggesting that swing-phase limb dynamics may play an important role in the stabilization of running animals.

Key words: biomechanics, legged locomotion, return map, spring-mass model, swing phase.

Introduction

In running, kinetic and potential energy removed from the body during the first half of a running step is transiently stored as elastic strain energy and later released during the second half by elastic recoil. The mechanism of elastic recoil was first proposed in 1964, when Cavagna and collaborators noticed that the forward kinetic energy of the body's center of mass is in phase with fluctuations in gravitational potential energy (Cavagna et al., 1964). They hypothesized that humans and animals most likely store elastic strain energy in muscle, tendon, ligament and perhaps even bone to reduce fluctuations in total mechanical energy. Motivated by these energetic data, Blickhan (1989) and McMahon and Cheng (1990) proposed a simple model to describe the stance period of symmetric running gaits: a point mass attached to a massless, linear spring. Using animal data to select the initial conditions at first ground contact, they demonstrated that the spring-mass model can predict important features of stance period dynamics (Blickhan, 1989; McMahon and Cheng, 1990).

Since its formulation the spring-mass model has served as the basis for theoretical treatments of animal and human running, not only for the study of running mechanics, but also stability. Kubow and Full (1999) investigated the stability of hexapod running in numerical simulation. At a preferred forward velocity, a pre-defined sinusoidal pattern of each leg's ground reaction force resulted in stable movement patterns.

However, the legs could not be viewed as entirely spring-like since their force production did not change in response to disturbances applied to the system. Later Schmitt and Holmes (2000) found a lateral spring-mass stability for hexapod running on a conservative level where total mechanical energy is constant. However, in this study, they investigated lateral and not sagittal plane stability in a uniform gravitational field. In contrast, Seyfarth et al. (2002) investigated the stride-to-stride sagittal plane stability of a spring-mass model. Although the model is conservative it can distribute its energy into forward and horizontal directions by selecting different leg angles at touch-down (Geyer et al., 2002). Surprisingly, this partitioning turns out to be asymptotically stable and predicts human data at moderate running speeds (5 m s^{-1}). However, model stability cannot be achieved at slow running speeds ($\leq 3 \text{ m s}^{-1}$). Additionally, at moderate speeds ($\sim 5 \text{ m s}^{-1}$), a high accuracy of the landing angle ($\pm 1^\circ$) is required, necessitating precise control of leg orientation.

The purpose of this study is to investigate control strategies that enhance the stability of the spring-mass model on a conservative level. In the control scheme of Seyfarth et al. (2002), the angle with which the spring-mass model strikes the ground is held constant from stride-to-stride. In this investigation, we relax this constraint and impose a swing-leg retraction, a behavior that has been observed in running

humans and animals (Muybridge, 1955; Gray, 1968) in which the swing-leg is moved rearward towards the ground during late swing-phase. This controlled limb movement has been shown to reduce foot-velocity with respect to the ground and, therefore, landing impact (De Wit et al., 2000). Additionally, a biomechanical model for quadrupedal locomotion indicated that leg retraction could improve stability in quadrupedal running (Herr, 1998; Herr and McMahon, 2000, 2001; Herr et al., 2002). We hypothesize that swing-leg retraction improves the stability of the spring-mass model by automatically adjusting the angle with which the model strikes the ground from one stride to the next. We test this hypothesis by imposing a constant rate of retraction throughout the second half of the swing phase. Using a return map analysis on swing-phase apex height (Seyfarth et al., 2002), we compare model stability at zero retraction velocity (constant angle of attack) to model stability at several non-zero retraction velocities.

Materials and methods

Spring-mass running with leg retraction

Running is characterized by a sequence of contact and flight phases. For the contact phase of symmetric running gaits, researchers have described the dynamics of the center of mass with a spring-mass model comprising a point mass attached to a massless, linear leg spring (Blickhan, 1989; McMahon and Cheng, 1990). To describe the dynamics of the flight phase, a ballistic representation of the body's center of mass has been used (McMahon and Cheng, 1990). In their investigation of the stability of spring-mass running, Seyfarth et al. (2002) assumed that the leg spring strikes the ground at a fixed angle with respect to the ground.

In this investigation, the effect of swing-leg retraction on the stability of the spring-mass model is investigated. Here the orientation of the leg is not held fixed during the swing phase, but is now considered a function of time $\alpha(t)$. For simplicity, we assume a linear relationship between leg angle (measured with respect to the horizontal) and time, starting at the apex t_{APEX} with an initial leg angle α_R (retraction angle) (Fig. 1):

$$\text{for } t < t_{\text{APEX}}, \quad \alpha(t) = \alpha_R, \quad (1a)$$

$$\text{for } t \geq t_{\text{APEX}}, \quad \alpha(t) = \alpha_R + \omega_R(t - t_{\text{APEX}}), \quad (1b)$$

where ω_R is a constant angular leg velocity (retraction speed).

Stability analysis

To evaluate the stability of potential movement trajectories, we use a return map analysis. For legged locomotion, a return map relates the system state at a characteristic event or moment within a gait cycle to the system state at the same event or moment one period later. To keep the analysis as simple as possible, we select the swing-phase apex height as the characteristic event. At this point, the system state $(x, y, v_x, v_y)_{\text{APEX}}$ is uniquely identified by one variable, the apex height y_{APEX} . Here, x and y are the horizontal and vertical positions, and v_x and v_y are the horizontal and vertical velocities of the

model's point mass. The system state is uniquely defined by the apex height due to (1) the vanishing vertical velocity $v_{y,\text{APEX}}=0$ at this point, (2) the fact that x has no influence on future periodic behavior, and (3) the conservative nature of the spring-mass system in which total mechanical energy is held constant.

The return map investigates how this apex height changes from step to step, or more precisely, from one apex height (index ' i ') to the next one (index ' $i+1$ ') in the following flight phase (after one contact phase). For a stable movement pattern, two conditions must be fulfilled within this framework: (1) there must be a periodic solution (Equation 2a, called a fixed point where y_{APEX}^* is the steady state apex height), and (2) deviations from this solution must diminish step-by-step (Equation 2b, or an asymptotically stable fixed point).

$$y_{i+1} = y_i = y_{\text{APEX}}^*, \quad (2a)$$

$$\text{where} \quad \left| \frac{dy_{i+1}}{dy_i} \right|_{y_{\text{APEX}}^*} < 1. \quad (2b)$$

For simplicity, the subscript APEX in y_{i+1} and y_i has been removed.

The requirements for stable running can be checked graphically by plotting a selected return map (e.g. for a given retraction angle α_R and a given retraction velocity ω_R) within the (y_i, y_{i+1}) plane and searching for stable fixed points fulfilling both conditions defined by Equations 2a and 2b. The first condition (Equation 2a, periodic solutions) requires that there is a solution (i.e. a single point) of the return map $y_{i+1}(y_i)$ located at the diagonal $(y_{i+1}=y_i)$. The second condition (Equation 2b, asymptotic stability) demands that the slope (dy_{i+1}/dy_i) of the return map $y_{i+1}(y_i)$ at the periodic solution (intersection with the diagonal) is neither steeper than 1 (higher than 45°) nor steeper than -1 (smaller than -45°).

As a consequence of the imposed leg retraction, the return map of the apex height $y_{i+1}(y_i)$ is determined by two mechanisms: the control of the angle of attack $\alpha_0(y_i)$ before landing (leg retraction) and the dynamics of the spring-mass model resulting in the next apex height $y_{i+1}(\alpha_0, y_i)$. According to the definition of leg retraction (Equation 1), the analytical relationship between the apex height y_{APEX} and the landing angle of attack α_0 is:

$$y_{\text{APEX}}(\alpha_0) = l_0 \sin \alpha_0 + \frac{g}{2} \left(\frac{\alpha_0 - \alpha_R}{\omega_R} \right)^2. \quad (3)$$

where l_0 denotes the leg length at touch-down and g is the vertical component of the gravitational acceleration. Merely one branch of the quadratic function in α_0 has to be considered as retraction holds only for times $t \geq t_{\text{APEX}}$ according to Equation 1 (either $\alpha_0 > \alpha_R$ or $\alpha_0 < \alpha_R$, depending on the sign of ω_R). This allows us to derive the control strategy $\alpha_0(y_{\text{APEX}})$.

Numerical procedure

The running model is implemented in Simulink (Mathworks) using a built-in variable time step integrator

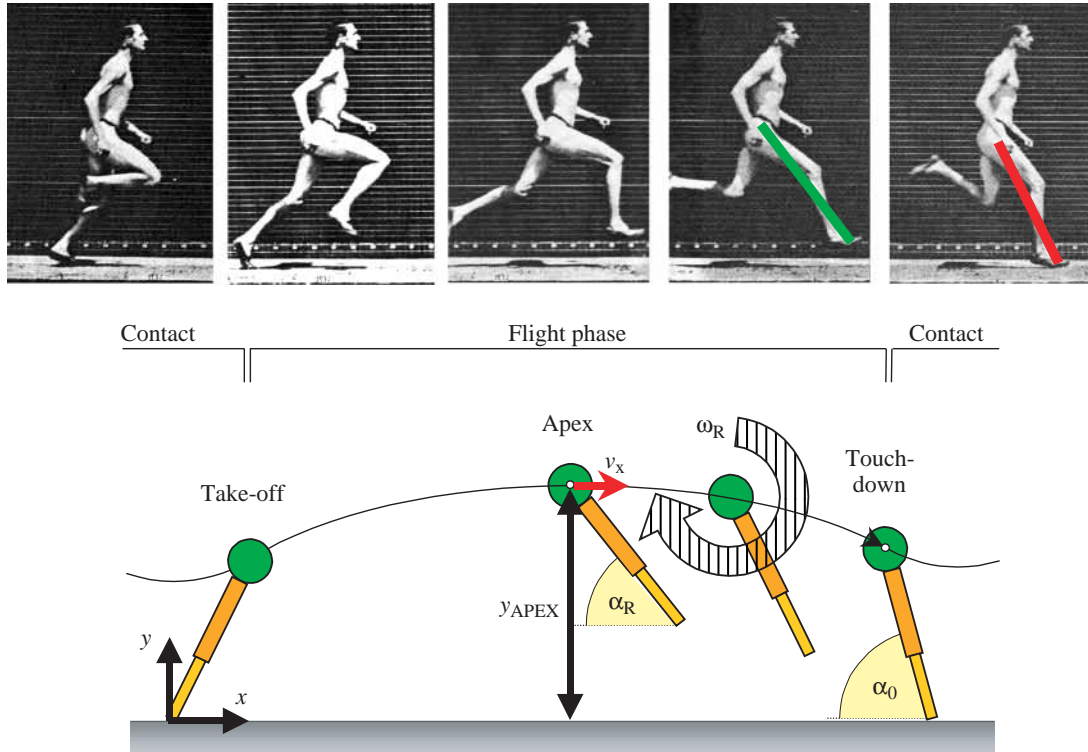


Fig. 1. Spring-mass model with retraction. Swing-leg retraction in running, as indicated by the photographs of Muybridge (1955; reproduced with permission from Dover Publications), is modeled assuming a constant rotational velocity of the leg (retraction speed ω_R), starting at the apex of the flight phase at retraction angle α_R . Depending on the duration of the flight phase, the landing angle of the leg (angle of attack α_0) is a result of the model dynamics and has no predefined constant value in contrast to the previous model of Seyfarth et al. (2002). The axial leg operation during the stance phase is approximated by a linear spring of constant stiffness k_{LEG} .

(ode113) with a relative tolerance of $1e-12$. For a human-like model (point mass $m=80$ kg, leg length $l_0=1$ m) at different horizontal speeds v_x (initial conditions at apex $y_{0,APEX}$ are $v_{x,APEX}=v_x$ and $v_{y,APEX}=0$), the leg parameters (k_{LEG} , α_R , ω_R) for stable running are identified by scanning the parameter space and measuring the number of successful steps. The stability of potential solutions is evaluated using the return map $y_{i+1}(y_i)$ of the apex height y_{APEX} of two subsequent flight phases (i and $i+1$). For a given system energy E , all possible apex heights $0 \leq y_{0,APEX} \leq E/(mg)$ are taken into account. For instance, for a system energy E corresponding to an initial horizontal velocity $v_x=5$ m s $^{-1}$ at an apex height $y_{0,APEX}=1$ m, apex heights between 0 and 2.27 m are taken into account. To keep the system energy constant, the horizontal velocity at apex $v_{0,APEX}=v_x$ is adjusted according to the selected apex height $y_{0,APEX}$ using the equation $mg y_{0,APEX} + m/2(v_{0,APEX})^2 = E$.

Results

Can leg retraction stabilize spring-mass running?

The kinematics of the spring-mass model are evaluated using (1) a fixed angle of attack α_0 and (2) the swing-leg retraction strategy (Equation 1). The results are shown in Fig. 2. Starting at an initial apex height of 1.25 m, both control strategies stabilize to a final limit cycle. Spring-mass running

with a fixed angle of attack α_0 is stable if (1) the leg stiffness k_{LEG} and the angle of attack α_0 are both properly adjusted to the chosen running speed and (2) the initial vertical position $y_{0,APEX}$ is within the range of attraction for the corresponding stable fixed point. (For more information on spring-mass running using a fixed angle of attack, see Seyfarth et al., 2002).

With the swing-leg retraction control, the rotational leg velocity before landing (retraction speed ω_R) leads to a step-to-step adjustment of the angle of attack α_0 , which gradually converges to a final steady state angle α_0^* (dotted line in Fig. 2C). Since the leg has a fixed angular velocity during the second half of the flight phase, the chosen initial apex height ($y_{0,APEX}=1.25$ m) leads to a steeper landing angle compared to the steady state angle α_0^* . Consequently, the first contact phase is asymmetric with respect to the vertical axis (Fig. 2A,C) and therefore, the next apex height is lower than the previous apex height. Due to the shorter flight phase, the second angle of attack is clearly flatter (a smaller angle of attack). Finally, the system stabilizes at the steady state angle α_0^* with a corresponding apex height y_{APEX}^* .

With leg retraction, steady-state running is achieved within approximately 2 steps, whereas the system without retraction needs approximately 8 steps (Fig. 2A). This indicates that leg retraction can improve the attraction of stable limit cycles in running.

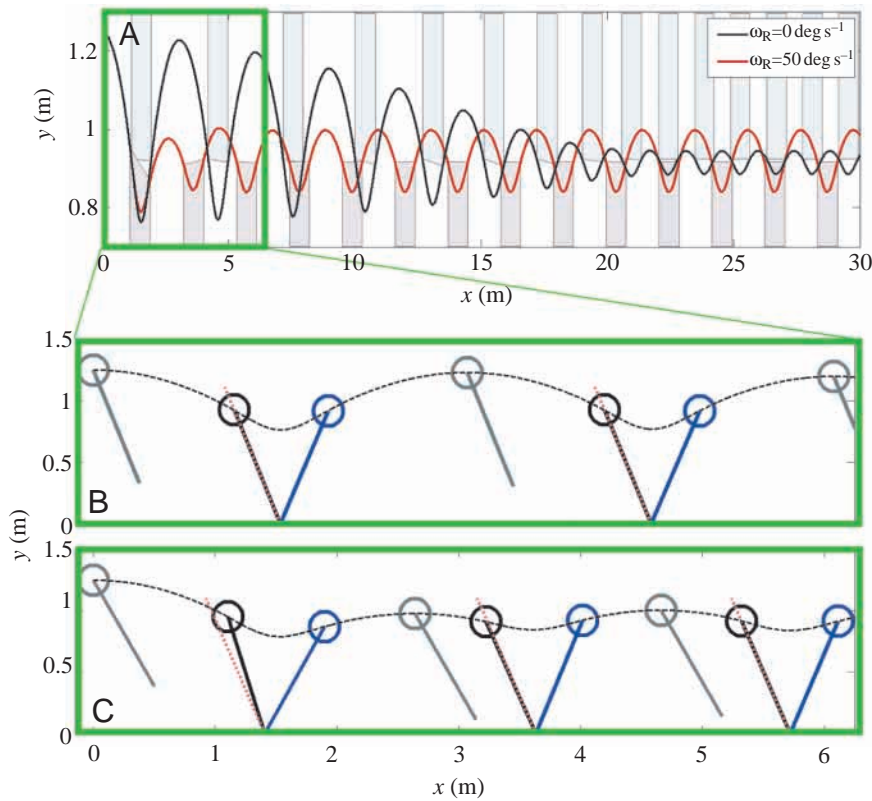


Fig. 2. Center of mass trajectories (A) and leg kinematics (B,C) for spring-mass running with and without retraction (C, $\omega_R=50 \text{ deg s}^{-1}$; B, $\omega_R=0 \text{ deg s}^{-1}$). The bars in A indicate the change in centre of mass height between touch-down and take-off. B and C are expanded views of plot A from 0 to 6 m (boxed). For each simulated run, the same initial apex height was used ($y_0=1.25 \text{ m}$), and for the simulation with retraction, a retraction angle of $\alpha_R=60^\circ$ was assumed (C). Here the model with retraction reached a steady state condition after two steps in contrast to approximately 8 steps for the model without retraction (A,B). The red dotted lines in B and C denote the steady state landing angle α_0^* .

Stability analysis for running

The influence of leg retraction on the return map of the apex height is shown in Fig. 3. With increased retraction speed ($\omega_R=25$ and 50 deg s^{-1}) the solutions of $y_{i+1}(y_i)$ for different retraction angles α_R become more horizontally aligned. As a consequence, disturbances in apex height are compensated for more rapidly (paths

indicated by the arrows in Fig. 3). Furthermore, the attraction range in y_{APEX} for the stable fixed points is largely increased (maximum increase in y_{APEX} : $\sim 35 \text{ cm}$ for $\omega_R=0$, $\sim 90 \text{ cm}$ for $\omega_R=25 \text{ deg s}^{-1}$, and $\sim 120 \text{ cm}$ for $\omega_R=50 \text{ deg s}^{-1}$. See dotted lines in Fig. 3).

In the case of leg retraction, the control of the angle of attack α_0 is shifted into a control of the retraction angle α_R . For zero retraction speed ($\omega_R=0$) the retraction angle α_R becomes identical to the angle of attack α_0 ($\alpha_R=\alpha_0$, Fig. 3A), i.e. the leg angle is adjusted at apex height and does not change until ground contact. With increasing retraction speed ω_R , the range of retraction angles resulting in stable running is enlarged (2.6° for $\omega_R=0$; 7.2° for $\omega_R=25 \text{ deg s}^{-1}$; 14.6° for $\omega_R=50 \text{ deg s}^{-1}$).

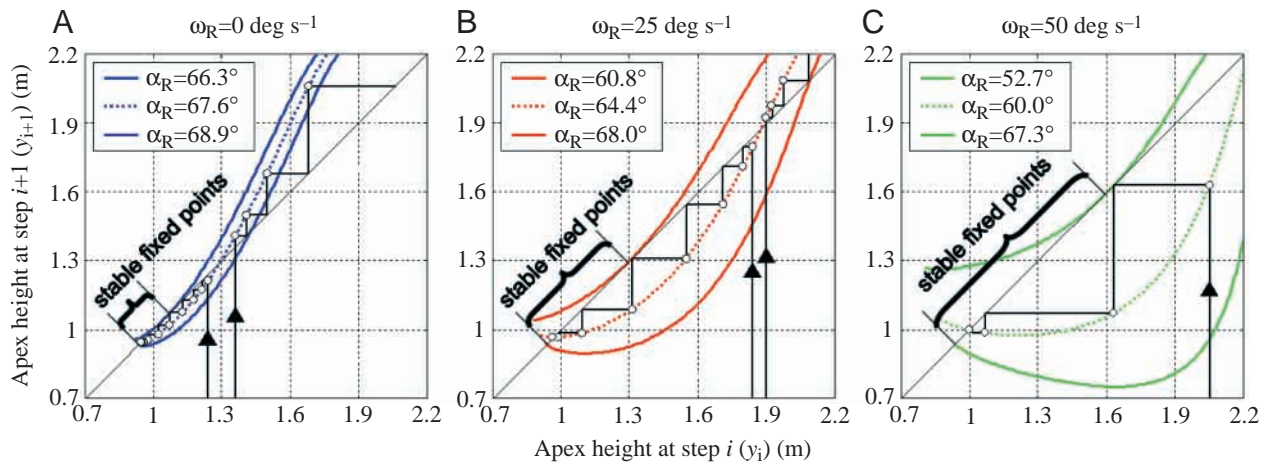


Fig. 3. Return maps $y_{i+1}(y_i)$ of the apex height y_{APEX} of two consecutive flight phases (index i and $i+1$) for three different retraction speeds ω_R (A, $\omega_R=0 \text{ deg s}^{-1}$; B, $\omega_R=25 \text{ deg s}^{-1}$; C, $\omega_R=50 \text{ deg s}^{-1}$). The system energy corresponds to a running speed of 5 m s^{-1} at an apex height $y_{APEX}=1 \text{ m}$. (A–C) Three characteristic return maps represent the minimum, mean and maximum retraction angle α_R (see key in each panel) for stable fixed points (see text, Equation 2). With increasing retraction speed ω_R , the range of retraction angles α_R with stable fixed points increases, and attraction of higher apex heights is observed (max. $y_0 \approx 1.3, 1.9, 2.2$ for $\omega_R=0, 25, 50 \text{ deg s}^{-1}$, respectively) as shown by representative tracings (running sequences are indicated by stepped black lines with starting arrows).

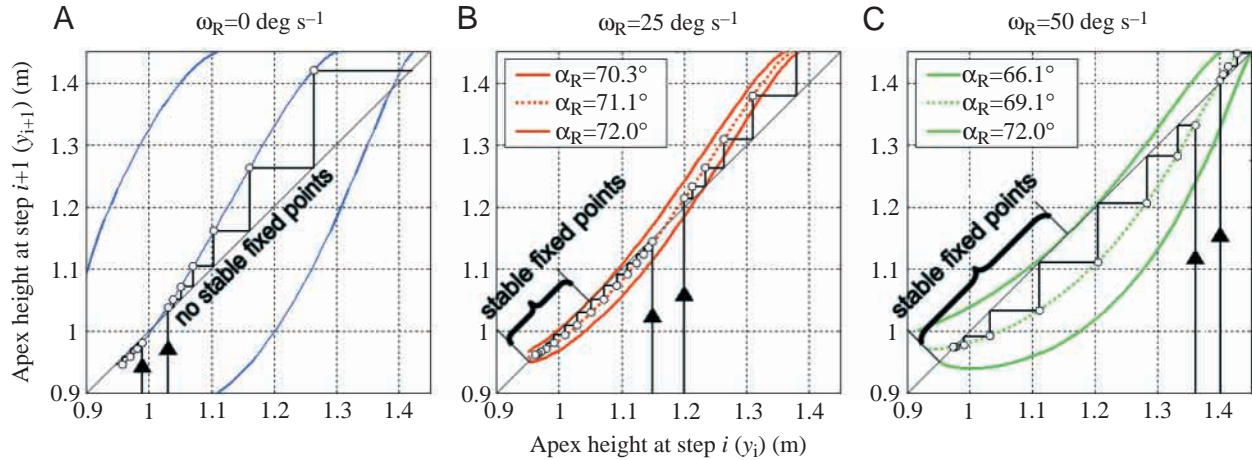


Fig. 4. Return maps $y_{i+1}(y_i)$ of the apex height y_{APEX} are shown for different retraction speeds ω_R (A, $\omega_R=0$ deg s^{-1} ; B, $\omega_R=25$ deg s^{-1} ; C, $\omega_R=50$ deg s^{-1}) but for a lower system energy corresponding to a slower running speed of 3 m s^{-1} at an apex height $y_{APEX}=1$ m. Stable fixed points require non-zero retraction velocities $\omega_R>0$ (B,C). As in Fig. 3, an increased retraction speed leads to an enlarged attraction of the stable fixed points with respect to a given initial (e.g. disturbed) apex height. Model parameters: $m=80$ kg, $l_0=1$ m, $k_{LEG}=20$ kN m^{-1} .

Running at low speeds

Spring-mass running with a fixed angle of attack is characterized by a minimum speed required for stability (Seyfarth, 2002). In Fig. 4, a running speed ($v_X=3$ m s^{-1}) close to this minimum speed is selected. At the given leg stiffness ($k_{LEG}=20$ kN m^{-1}) no stable fixed point exists without retraction (Fig. 4A). Employing the leg retraction control, stable fixed points emerge in the return map. Similar to the finding in Fig. 3, an increased retraction speed ω_R leads to (1) an enlarged range of attraction in y_{APEX} , (2) a faster convergence to the stable fixed point (fewer steps), and (3) an increased range of successful retraction angles α_R for stable running.

Robustness with respect to leg stiffness k_{LEG}

Spring-mass running requires a proper adjustment of leg stiffness to the chosen angle of attack (Blickhan, 1989; McMahon and Cheng, 1990; Herr and McMahon, 2000, 2001; Seyfarth, 2002). However, even at zero retraction speed ($\omega_R=0$), a range of leg stiffness can fulfill periodic running at a given angle of attack α_0 (Seyfarth, 2002). To test the robustness of spring-mass running with respect to variations in leg stiffness, we estimate the maximum and minimum stiffness change that could be tolerated by the system. A stiffness change is applied during steady state running, starting from an initial leg stiffness of 20 kN m^{-1} (Fig. 5A). For these numerical experiments, the mean angles of attack ($\alpha_R=67.6^\circ$, 64.4° , 60.0° in Fig. 5A,C,E) with respect to the range of all α_R with stable fixed points in Fig. 3A–C are used. After the first three steps in steady state running, leg stiffness is permanently shifted. Without retraction, variations in leg stiffness within 18.2 and 22.4 kN m^{-1} are tolerated (Fig. 5A) even without any stride-to-stride adaptations in the angle of attack (Fig. 5B).

By introducing leg retraction (Fig. 5C, $\omega_R=25$ deg s^{-1} ;

Fig. 5E, $\omega_R=50$ deg s^{-1}), the range of tolerated stiffness is largely increased (16 – 28.8 kN m^{-1} for $\omega_R=25$ deg s^{-1} ; 13.9 – 62 kN m^{-1} for $\omega_R=50$ deg s^{-1}). These results show that the rotational velocity of the leg ω_R inherently adapting the angle of attack α_0 allows for large variations in leg stiffness (Fig. 5D,F).

Discussion

Late swing-phase retraction has been observed in running animals of different leg number and body size (Muybridge, 1955; Gray, 1968). Although swing-leg retraction seems to be a general feature in biological running, few researchers (De Wit et al., 2000; Herr and McMahon, 2000, 2001; Herr et al., 2002) have studied the behavior and, consequently, its purpose is not fully understood. In this investigation, we show that leg retraction is a simple strategy to improve the stability of spring-mass running. By imposing a uniform retraction velocity, we demonstrate that the stability of the spring-mass model is increased with respect to variations in forward speed, leg angle (retraction angle α_R) and leg stiffness k_{LEG} .

Swing-leg retraction approximates the natural angle of attack

In terms of the return map of the apex height, we can ask for an ‘optimal’ control strategy by imposing the constraint $y_{i+1}(y_i)=y_{CONTROL}=\text{constant}$. Within one step this return map projects all possible initial apex heights y_i to the desired apex height $y_{i+1}=y_{CONTROL}$.

As a consequence of the dynamics of the spring-mass system, the apex height y_{i+1} is merely determined by the preceding apex height y_i and the selected angle of attack α_0 . This dependency $y_{i+1}(y_i, \alpha_0)$ can be understood as a ‘fingerprint of spring-like leg operation’ and is represented as a surface in Fig. 6A. When applying any control strategy $\alpha_0(y_i)$, this

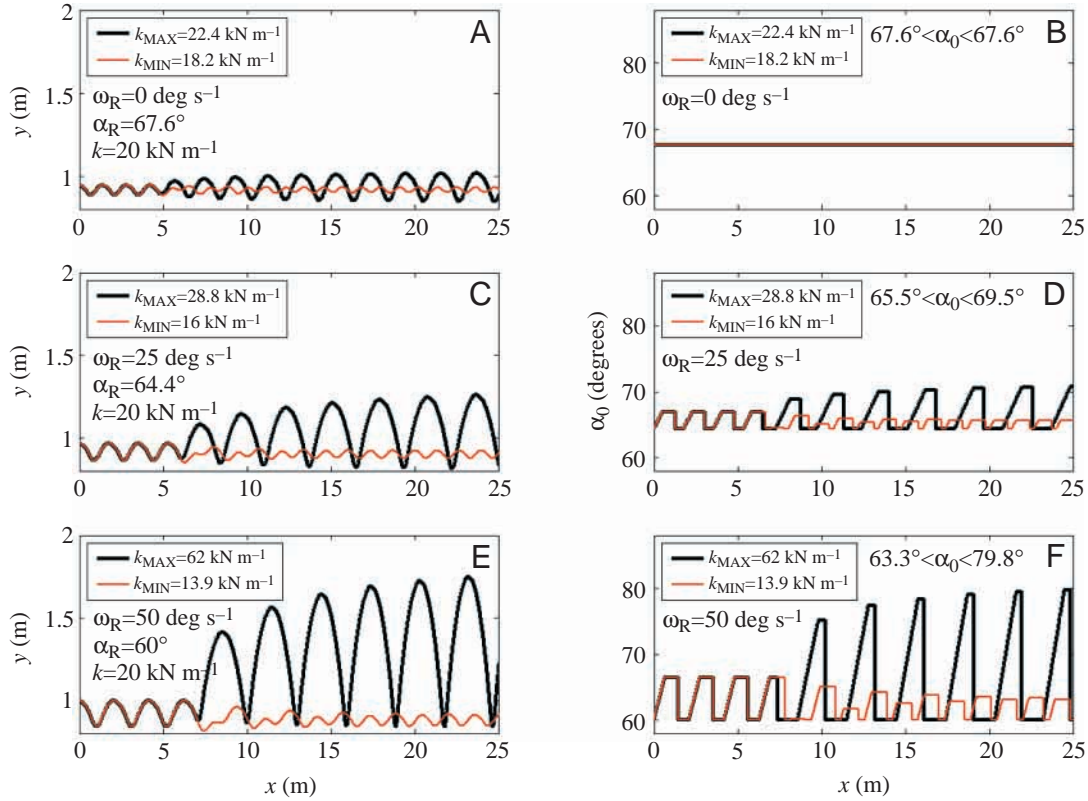


Fig. 5. The influence of retraction speed ω_R on the robustness of running is shown with respect to a permanent change in leg stiffness k_{LEG} . For each run ($v_{x,0}=5 \text{ m s}^{-1}$, $y_0=1 \text{ m}$), the maximum and minimum leg stiffness (k_{MIN} , k_{MAX}) required to keep the system in a periodic running movement are depicted (A,C,E). The retraction angle α_R (denoted in A,C,E) is chosen according to the mean retraction angle for stable fixed points in Fig. 3 at $k_{LEG}=20 \text{ kN m}^{-1}$. (B,D,F) The adaptation of the leg angle to the changed leg stiffness.

generalized surface $y_{i+1}(y_i, \alpha_0)$ can be used to derive the corresponding return maps.

For example, in the case of a ‘fixed angle of attack’ (no retraction: $\alpha_0(y_i)=\alpha_R=\text{constant}$) the surface has to be scanned at lines of constant angles α_0 (Fig. 6A, e.g. red line: $\alpha_0=68^\circ$). These lines are projected to the left (y_{i+1}, y_i) plane in Fig. 6A and match the return map in Fig. 3A.

Let us now consider the ‘optimal control strategy for stable running’ $\alpha_0(y_i)$ fulfilling $y_{i+1}(y_i)=y_{CONTROL}=\text{constant}$. Using the identified fingerprint, this simply requires us to search for isolines of constant y_{i+1} on the generalized surface $y_{i+1}(y_i, \alpha_0)$, as indicated by the green lines in Fig. 6A ($y_{i+1}=1, 1.5$ and 2 m). The projection of these isolines onto the (α_0, y_i) plane represents the desired ‘natural’ control strategy $\alpha_0(y_i)$ for spring-mass running as depicted for $y_{CONTROL}=1, 1.5, 2 \text{ m}$ in Fig. 6B.

The constant-velocity leg retraction model put forward in this paper represents a particular control strategy $\alpha_0(y_i)$ relating the angle of attack α_0 to the apex height y_i of the preceding flight phase (Equation 3), as shown in Fig. 6B for different retraction speeds ($\omega=0, 25, 50, 75 \text{ deg s}^{-1}$) and one retraction angle ($\alpha_R=60^\circ$). It turns out that this particular leg retraction model can approximate the natural control strategy within a considerable range of apex heights if the proper retraction parameters (α_R, ω_R) are selected. The value of the retraction angle α_R shifts the line of the retraction control $\alpha_0(y_i)$ along

the α_0 axis, whereas the retraction speed ω_R determines the slope of the control line. Thus, the retraction parameters have different qualities with respect to the control of running; if the retraction speed ω_R guarantees the stability (setting the range and the strength of attraction to a fixed point), then the retraction angle α_R selects the apex height of the corresponding fixed point $y_{CONTROL}$. Due to this adaptability, a constant velocity leg retraction model, as evaluated in this paper, can significantly enhance the stability of running compared to the fixed angle control model described by Seyfarth et al. (2002).

Influence of speed on the stability of spring-mass running

The return maps in Figs 3 and 4 indicate that the generalized surface $y_{i+1}(y_i, \alpha_0)$ is a function of the forward running speed. The selected retraction speeds in Figs 3 and 4 ($\omega_R=0, 25, 50 \text{ deg s}^{-1}$) show that the slope of the return map $y_{i+1}(y_i)$ generally increases with (1) decreasing running speed and (2) decreasing retraction speed ω_R . As a consequence, running at 3 m s^{-1} is not stable using a fixed angle of attack ($\omega_R=0$ in Fig. 4A), but is stable using non-zero retraction speeds ($\omega_R=25$ and 50 deg s^{-1} in Fig. 4B and C, respectively). Hence, even at slow forward running speeds ($\leq 3 \text{ m s}^{-1}$), there exists a natural control strategy represented by the isolines of the corresponding generalized surface with $y_{i+1}(y_i, \alpha_0)=\text{constant}$. In comparison with the fixed angle of attack control, leg

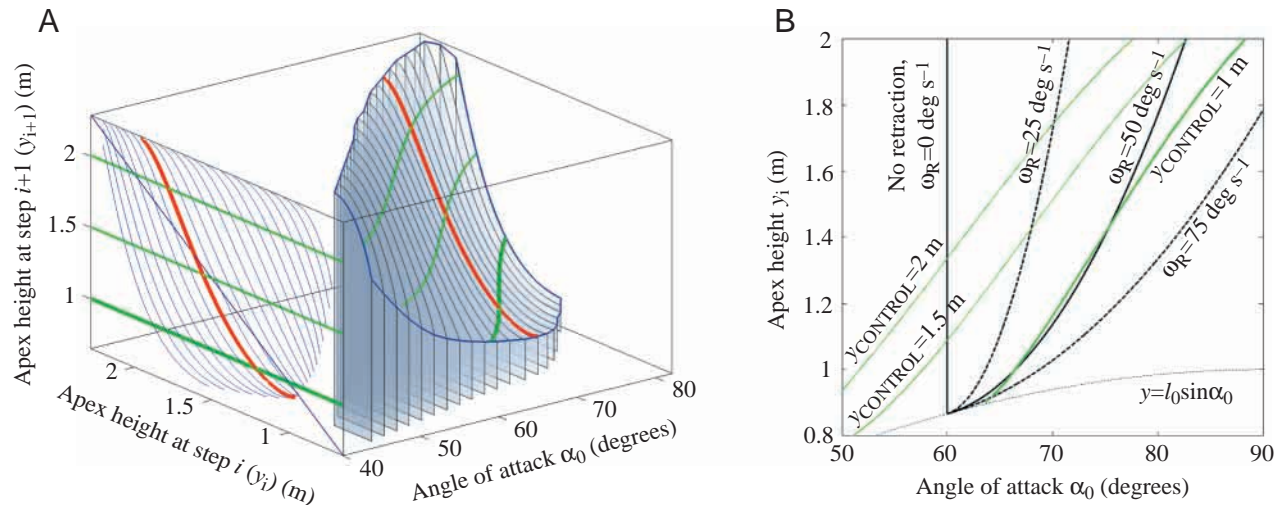


Fig. 6. (A) A three-dimensional (3D) representation $y_{i+1}(y_i, \alpha_0)$ of the return map $y_{i+1}(y_i)$ characterizes spring-mass running (system energy corresponds to $v_X=5$ m s $^{-1}$ at $y_{APEX}=1$ m; $m=80$ kg, $l_0=1$ m, $k=20$ kN m $^{-1}$) for different angles of attack α_0 . For fixed angles of attack (slices in 3D), the corresponding return maps are shown on the left (y_i, y_{i+1}) plane. The red line depicts the return map for $\alpha_0=68^\circ$. Different return maps are possible if the angle of attack α_0 becomes dependent on the apex height y_i . An ‘optimal’ control model with respect to stability would be a direct projection of any initial apex height y_i to a desired apex height $y_{CONTROL}$ in the next flight phase, or $y_{i+1}(y_i)=y_{CONTROL}=\text{constant}$, as shown for apex heights of 1, 1.5 and 2 m (left plane). This corresponds to isolines on the 3D-surface $y_{i+1}(y_i, \alpha_0)$ indicating a dependency between the angle of attack α_0 and the initial apex height y_i , as shown for $y_{CONTROL}=1, 1.5$ and 2 m in (B). With careful selection of the retraction velocity ω_R and the retraction angle α_R , the constant velocity leg retraction model can approximate the optimal control strategy.

retraction at constant velocity approximates this natural control (Fig. 6B). Thus, a constant velocity retraction is a successful strategy to stabilize running below the critical forward running speed where stable running is not achievable using a fixed angle control.

The fact that the spring-mass model, with retraction, is stable at slow forward running speeds seems critical. Clearly, for a running model to be viewed as a plausible biological representation, the model should be stable across the full range of biological running speeds. Without swing-leg retraction, the spring-mass model could not be stabilized at slow biological running speeds (~ 3 m s $^{-1}$ for $m=80$ kg, $l_0=1$ m, $k_{LEG}=20$ kN m $^{-1}$; Fig. 4A), but with retraction, the spring-mass model could readily be stabilized (Fig. 4B,C).

Swing-leg retraction in human running: preliminary experimental results

A treadmill (Woodway, Germany) was equipped with an obstacle-machine designed to disturb swing-phase dynamics during human running. The obstacle-machine consisted of a cylindrical-shaped bar (2.5 cm diameter, 40 cm length) passing from the left to the right side of the treadmill walkway (the bar’s long axis is generally perpendicular to the direction of the moving treadmill surface). Every 9–16 s, the bar moved towards the human runner at a speed equivalent to the treadmill surface, forcing the runner to change his swing-phase kinematics to avoid the obstacle. The movement of the obstacle bar was triggered by the ground reaction force F . For each experiment, the bar was positioned 12 cm above the moving treadmill surface.

Using this apparatus, we conducted experiments on five male subjects (body mass 79.6 ± 5.9 kg, age 30.6 ± 3.2 yrs) performing treadmill running at 3 m s $^{-1}$. We measured leg kinematics (leg angle, leg length) during both the stance and swing phases. Leg angle α and length l_{LEG} at the onset of swing-leg retraction and at touch-down were used to characterise the kinematic leg control prior to landing. The retraction velocity ω_R was estimated as the mean angular velocity within the last 20 ms before touch-down. Furthermore, the leg stiffness k_{LEG} was approximated using the maximum vertical ground reaction force F_{MAX} and the maximum leg compression $\Delta l_{MAX}=\max(l_0-l)$ during stance phase with $k_{LEG}=F_{MAX}/\Delta l_{MAX}$.

For undisturbed running, we found surprisingly uniform leg kinematics during both the stance and swing phases (shown for one subject in Fig. 7). In contrast, when passing over the obstacle, swing-leg kinematics were altered significantly, but stance period dynamics immediately following the obstacle were largely unaffected. Swing-leg retraction was observed in undisturbed running with an angular range equal to $\alpha_{SHIFT}=4.5\pm 0.9^\circ$ (Table 1). During this period of swing-leg retraction, only a minor change in leg length was observed ($l_{SHIFT}=1\pm 0.5$ cm), supporting one of the assumptions of our control model.

We observed a significant re-adjustment of leg retraction in response to the disturbance. Both the retraction angular range α_{SHIFT} ($\Delta\alpha_{SHIFT}=4.7\pm 3.0^\circ$, $P<0.05$, paired t -test) and the retraction velocity ω_R ($\Delta\omega_R=22\pm 13$ deg s $^{-1}$, $P<0.05$) increased in response to the disturbance. Here, the change in the angular range $\Delta\alpha_{SHIFT}$ was primarily the result of a decreased retraction

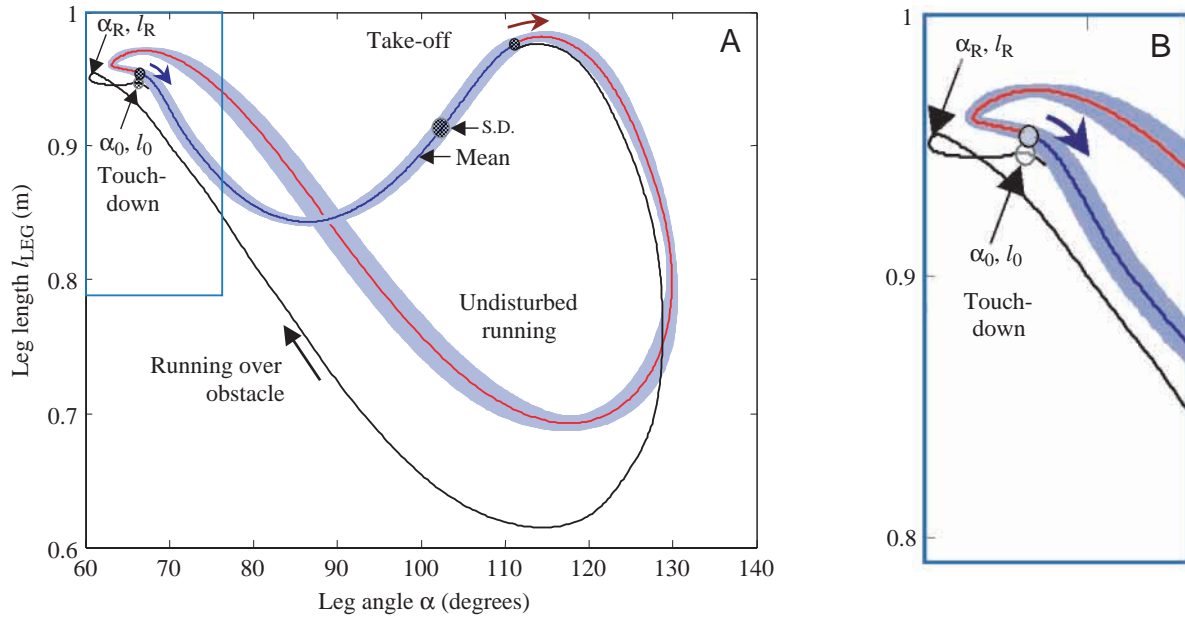


Fig. 7. Leg kinematics (leg length *versus* leg angle) during treadmill running at 3 m s^{-1} . For the undisturbed condition, the mean \pm S.D. of 35 running steps for one male subject (78 kg) are shown (A). The leg length l_{LEG} was measured as the distance between hip and toe marker. The leg angle α is defined as the projection angle with respect to the ground (Fig. 1). Swing-leg retraction is present between the onset angle α_{R} (length l_{R}) and the angle of attack α_0 (length l_0) as shown magnified in (B). For the disturbed swing phase, the leg operation of the same experimental subject is plotted. Although only a single subject is depicted here, similar results were observed in all experimental subjects (see Table 1).

Table 1. *Obstacle running*

	k_{LEG} (kN m^{-1})	α_0 (degrees)	α_{R} (degrees)	α_{SHIFT} (degrees)	ω_{R} (deg s^{-1})	l_0 (m)	l_{R} (m)	l_{SHIFT} (m)
Undisturbed running	25.2 ± 6.8	68.8 ± 2.1	64.3 ± 2.0	4.5 ± 0.9	137 ± 9	0.932 ± 0.020	0.942 ± 0.018	-0.010 ± 0.005
Disturbed running	22.9 ± 3.6	70.4 ± 2.7	61.3 ± 1.5	9.1 ± 3.6	159 ± 21	0.949 ± 0.018	0.959 ± 0.017	-0.010 ± 0.011
Difference (disturbed – undisturbed)	-2.3 ± 4.4	1.7 ± 2.1	-3.0 ± 2.5	$4.7 \pm 3.0^*$	$22 \pm 13^*$	0.017 ± 0.021	0.017 ± 0.023	0 ± 0.010

Values are means \pm S.D. ($N=5$ subjects).

k_{LEG} , leg stiffness; α_0 , angle of attack; α_{R} , onset angle of retraction; $\alpha_{\text{SHIFT}} = \alpha_0 - \alpha_{\text{R}}$, angle swept during retraction; ω_{R} , retraction velocity (mean value of the last 20 ms before touch-down); l_0 , leg length at touch-down; l_{R} , leg length at onset of retraction; $l_{\text{SHIFT}} = l_0 - l_{\text{R}}$, the shift in leg length during retraction (see Fig. 7).

In the undisturbed condition, at least 39 steps are evaluated for each subject.

Between 3 and 4 disturbed steps are used during obstacle avoidance.

The leg stiffness is measured in the stance phase immediately following the disturbance.

Differences between undisturbed and disturbed data are evaluated for significance using a paired *t*-test ($*P < 0.05$).

angle α_{R} ($\Delta\alpha_{\text{R}} = -3.0 \pm 2.5^\circ$, $P = 0.057$) rather than an increased angle of attack α_0 ($\Delta\alpha_0 = 1.7 \pm 2.1^\circ$, $P = 0.15$). In contrast, no significant change was observed in leg stiffness ($\Delta k_{\text{LEG}} = -2.3 \pm 4.4 \text{ kN m}^{-1}$, $P = 0.31$) or in leg length adjustment ($\Delta l_{\text{SHIFT}} = 0 \pm 1.0 \text{ cm}$, $P = 1$) during the stance period immediately following the disturbance.

These results indicate that leg retraction is employed in human running and is even enhanced when an obstacle disturbance is applied. The data presented here support the hypothesis of the model, namely, that swing-leg retraction is a strategy used in running to select an angle of attack that sustains a desired movement pattern.

Alternative biological strategies to stabilize running

The analysis reveals that the stability of spring-mass running is highly sensitive to the angular velocity of the leg before landing. Although swing-leg retraction seems an important stabilizing mechanism, we cannot ignore the importance of alternative strategies that might also be crucial for stable running. For instance, researchers have shown that visual feedback plays an important role in obstacle avoidance and, therefore, in stabilizing the movement trajectory. Warren et al. (1986) investigated regulatory mechanisms to secure proper footing using visual perception in human running. In their investigation, subjects ran on a treadmill across irregularly

spaced foot-targets in order to effectively modulate step length and the vertical leg impulse during stance. Although their results suggest that vision is important for running stability, they do not specifically address the issue of how mechanical or neuro-muscular mechanisms may contribute when running over ground surfaces *without* footing constraints.

Intrinsic or 'preflex' leg stabilizing mechanisms may also be important for running stabilization. It is well established that the intrinsic properties of muscle leads to immediate responses to length and particularly velocity perturbations (Humphrey and Reed, 1983; Brown et al., 1995). In an analytical study, Wagner and Blickhan (1999) showed that a self-stabilizing oscillatory leg operation emerges if well-established muscle properties are adopted.

Furthermore, by modeling the dynamics of the muscle-reflex system, stable, spring-like leg operations can be achieved in numerical simulations of hopping tasks if positive feedback of the muscle force sensory signals (simulated Golgi organs) are employed (Geyer et al., in press). These results suggest that during cyclic locomotory tasks such as walking or running, the body could counteract disturbances even during a single stance period.

Future work

Here we argue that swing-leg retraction is one of many stabilizing strategies used in biological running. Our research suggests that both the control of stance leg dynamics and swing-leg movement patterns may be critically important for overall running stability in humans and animals.

Leg retraction is a feedforward control scheme, and therefore, can neither avoid obstacles nor place the foot at desired foot-targets. Rather, the scheme provides a mechanical 'background stability' that may relax the control effort for locomotory tasks. It remains for future research to understand to what extent environmental sensory information might allow for varied kinematic trajectories and an increase in the stabilizing effects of swing-leg retraction. Future investigations will also be necessary to fully understand the impact of late swing-leg retraction on running stability. To gain insight into the control scheme employed by running animals, we wish to compare the natural retraction control formulated in this paper to the actual limb movements of running animals. Furthermore, since the spring-mass model of this paper is two-dimensional, we wish to generalize retraction to three dimensions to address issues of body yaw and roll stability. And finally, we hope to test optimized retraction control schemes on legged robots to enhance their robustness to internal (leg stiffness variations) and external disturbances (ground surface irregularities).

Conclusion

In this paper we show that swing-leg retraction can improve the stability of spring-mass running. With retraction, the spring-mass model is stable across the full range of biological running speeds and can overcome larger disturbances in the angle of attack and leg stiffness. In the stabilization of running humans and animals, we believe both stance-leg dynamics and swing-leg rotational movements are important control features.

List of symbols

E	system energy
F	vertical ground reaction force
g	vertical component of the gravitational acceleration
i	index
k_{LEG}	leg stiffness
l	leg length
m	mass
t	time
v	velocity
x	horizontal position
y	vertical position
α_{R}	retraction angle
ω_{R}	retraction speed

This research was supported by an Emmy-Noether grant of the German Science Foundation (DFG) to A.S. (SE 1042/1) and a grant of the German Academic Exchange Service (DAAD) 'Hochschulonderprogramm III von Bund und Länder' to H.G. We also thank the Michael and Helen Schaffer Foundation of Boston, Massachusetts for their generous support of this research.

References

- Blickhan, R.** (1989). The spring-mass model for running and hopping. *J. Biomech.* **22**, 1217-1227.
- Brown, I. E., Scott, S. H. and Loeb, G. E.** (1995). 'Preflexes' – programmable, high-gain, zero-delay intrinsic responses to perturbed musculoskeletal systems. *Soc. Neurosci. Abstr.* **21**, 562.9.
- Cavagna, G. A., Saibene, F. P. and Margaria, R.** (1964). Mechanical work in running. *J. Appl. Physiol.* **19**, 249-256.
- De Wit, B., De Clercq, D. and Aerts, P.** (2000). Biomechanical analysis of the stance phase during barefoot and shod running. *J. Biomech.* **33**, 269-278.
- Geyer, H., Seyfarth, A. and Blickhan, R.** (in press). Positive force feedback in bouncing gaits. *Proc. R. Soc. Lond. B.*
- Geyer, H., Seyfarth, A. and Blickhan, R.** (2002). *Natural Dynamics of Spring-Like Running: Emergence of Selfstability*. Paris, France: CLAWAR.
- Gray, J.** (1968). *Animal Locomotion*. London, Great Britain: Weidenfeld and Nicolson.
- Herr, H. M.** (1998). A model of mammalian quadrupedal running. PhD thesis, Department of Biophysics, Harvard University, USA.
- Herr, H. M. and McMahon, T. A.** (2000). A trotting horse model. *Int. J. Robotics Res.* **19**, 566-581.
- Herr, H. M. and McMahon, T. A.** (2001). A galloping horse model. *Int. J. Robotics Res.* **20**, 26-37.
- Herr, H. M., Huang, G. and McMahon, T. A.** (2002). A model of scale effects in mammalian quadrupedal running. *J. Exp. Biol.* **205**, 959-967.
- Humphrey, D. R. and Reed, D. J.** (1983). Separate cortical systems for control of joint movement and joint stiffness: reciprocal activation and coactivation of antagonist muscles. *Adv. Neurol.* **39**, 347-372.
- Kubow, T. M. and Full, R. J.** (1999). The role of the mechanical system in control: a hypothesis of self-stabilization in hexapedal running. *Phil. Trans. R. Soc. Lond. B* **354**, 849-861.
- McMahon, T. A. and Cheng, G. C.** (1990). The mechanics of running: how does stiffness couple with speed? *J. Biomech.* **23**, 65-78.
- Muybridge, E.** (1955). *The Human Figure in Motion*. New York: Dover Publications Inc.
- Schmitt, J. and Holmes, P.** (2000). Mechanical models for insect locomotion: dynamics and stability in the horizontal plane-theory. *J. Biol. Cybern.* **83**, 501-515.
- Seyfarth, A., Geyer, H., Günther, M., and Blickhan, R.** (2002). A movement criterion for running. *J. Biomech.* **35**, 649-655.
- Wagner, H. and Blickhan, R.** (1999). Stabilizing function of skeletal muscles: an analytical investigation. *J. Theor. Biol.* **199**, 163-179.
- Warren, W. H., Jr, Young, D. S. and Lee, D. N.** (1986). Visual control of step length during running over irregular terrain. *J. Exp. Psychol. Hum. Percept. Perform.* **12**, 259-266.